PCCP

COMMUNICATION

View Article Online
View Journal | View Issue

Cite this: *Phys. Chem. Chem. Phys.*, 2016, **18**, 5905

Received 21st December 2015,
Accepted 19th January 2016

DOI: 10.1039/c5cp07866k

www.rsc.org/pccp

Stable water layers on solid surfaces†

Ying-Jhan Hong,[a] Lin-Ai Tai,[b] Hung-Jen Chen,[b] Pin Chang,[b] Chung-Shi Yang*[b] and Tri-Rung Yew*[a]

Liquid layers adhered to solid surfaces and that are in equilibrium with the vapor phase are common in printing, coating, and washing processes as well as in alveoli in lungs and in stomata in leaves. For such a liquid layer in equilibrium with the vapor it faces, it has been generally believed that, aside from liquid lumps, only a very thin layer of the liquid, *i.e.*, with a thickness of only a few nanometers, is held onto the surface of the solid, and that this adhesion is due to van der Waals forces. A similar layer of water can remain on the surface of a wall of a microchannel after evaporation of bulk water creates a void in the channel, but the thickness of such a water layer has not yet been well characterized. Herein we showed such a water layer adhered to a microchannel wall to be 100 to 170 nm thick and stable against surface tension. The water layer thickness was measured using electron energy loss spectroscopy (EELS), and the water layer structure was characterized by using a quantitative nanoparticle counting technique. This thickness was found for channel gap heights ranging from 1 to 5 μm. Once formed, the water layers in the microchannel, when sealed, were stable for at least one week without any special care. Our results indicate that the water layer forms naturally and is closely associated only with the surface to which it adheres. Our study of naturally formed, stable water layers may shed light on topics from gas exchange in alveoli in biology to the post-wet-process control in the semiconductor industry. We anticipate our report to be a starting point for more detailed research and understanding of the microfluidics, mechanisms and applications of gas–liquid–solid systems.

1. Introduction

The macroscopic behaviors of liquids on solid surfaces, such as those of coffee ring stains,[1,2] tears of wine,[3] lotus effects,[4–6] and capillary action, have been investigated. When the characteristic length scale is as small as a couple of millimeters, inertia and gravity yield to surface tension[7] and interface adhesion[8] between liquid and solid surfaces. At length scales of only a few microns, microfluidics reaches its lower limit but is still a considerable distance from nanofluidics.[9] We investigated fluid behavior at or below the 10 μm scale range, which approximates the average pore size of alveoli in lungs and stoma in leaves. For example, in a microchannel, a void can form when there is insufficient liquid to fill the entire volume. The void is sometimes referred to as a bubble when it is completely surrounded by liquid. Often, the smallest dimension of the microchannel is the gap height (defined in Fig. 1), which confines and shapes the void with channel walls. A residual layer of liquid may remain on the channel wall, held there by van der Waals forces, but this force is known to weaken quickly for distances between two substances larger than a few nanometers.[10] For microchannels, where the channel heights are typically much smaller than the channel widths and lengths, the total liquid surface can be reduced if some of the void is filled (or bridged) with liquid at the expense of the thickness of the liquid residue. Surface tension, which plays a major role at microscales, tends to reduce liquid layer thickness.

Liquid layers on solid surfaces are crucial in printing, washing and coating processes.[1] Previously reported thicknesses of such layers have been observed to be sub-nanometer (<1 nm) for water adsorbed on gold[11] or 1 nm when on silica,[12] and 10 nm for a water layer on a hydrophilic wall in which case this thickness resulted from an increase in the viscosity of the water that was induced by the hydrophilic wall.[13] A 140 nm-thick layer of liquid lining the alveoli in the lung of a rat was reported;[14] and this water layer was attributed to a surface-active material composed of phospholipids.[15,16] We here report the observation of stable water layers approximately 100 to 170 nm thick on bare silicon nitride surfaces. This range of thickness was found to persist for channel gaps whose heights ranged from 1 to 5 μm and regardless of the nanoparticle size and concentration. Once formed, the water layers in a sealed microchannel were stable

[a] *Department of Materials Science and Engineering, National Tsing-Hua University, No. 101, Sec. 2, Kuang-Fu Road Hsinchu, 30013, Taiwan. E-mail: tryew@mx.nthu.edu.tw*

[b] *Bio Materials Analysis Technology, 1F, No. 26-2, Tai-Yuen St. Jubei, Hsinchu County, 30288, Taiwan. E-mail: cyang@bioma-tek.com*

† Electronic supplementary information (ESI) available: More details on EELS analyses, and quantitative nanoparticle technique. See DOI: 10.1039/c5cp07866k

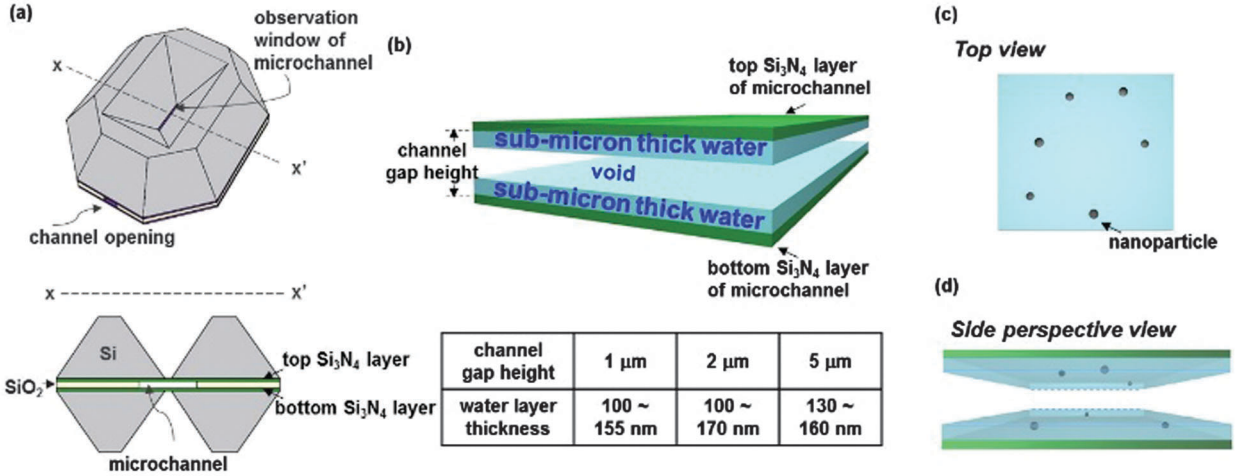

channel gap height	1 μm	2 μm	5 μm
water layer thickness	100 ~ 155 nm	100 ~ 170 nm	130 ~ 160 nm

Fig. 1 Schematics of (a) microchannels (K-kit) used in this work, (b) stable water layers with a void in between, and (c) top view and (d) side view of water layers with nanoparticle tracers illustrating the relationship between the observed nanoparticle area density and the water layer thickness.

without any special care for at least one week (Note that one week was the extent of our observation time.). We suggest that the Casimir–Lifshitz[17] force was responsible for maintaining the water layer against surface tension, though proving this suggestion is beyond the scope of the current study.

In addition to fluid manipulations in microfluidics, from gas exchange in alveoli in biology[18,19] to post-wet-process control in the semiconductor industry,[25,26] the possibility of forming and maintaining such a thick liquid layer on wall surfaces has not been considered in fields where such a stable sizable liquid layer would be important.

2. Experimental

2.1 Description of the microchannel used

We used a micro-electro-mechanical systems (MEMS) microchannel chip called K-kit, shown in Fig. 1(a). This liquid sample holder for transmission electron microscopy (TEM) was first developed by this group[20] and commercialized by Bio MA-Tek, who provided the K-kit in this study. The liquid channel used was 120 μm wide, approximately 1.5 mm long, with various channel gap heights available. In this study, we used channel gaps with heights of 1, 2, and 5 μm, measured from inside two observation windows made of 100 nm-thick Si_3N_4.

To remove organic or metallic contamination, the microchannels were cleaned by soaking them sequentially in acetone, ethanol, and deionized (DI) water for 5 min. Subsequently, the microchannels were cleaned with H_2SO_4/H_2O_2 (3 : 1 by volume, and with original H_2SO_4 and H_2O_2 concentrations of 97% and 30%, respectively) at 90 °C for 20 min, and then soaked thrice in DI water for 5 min to remove the H_2SO_4/H_2O_2. Finally, the microchannels were baked on a hot plate at 140 °C for 10 min, and then cooled at room temperature for 10 min.

The Si_3N_4 surface was highly hydrophilic after cleaning. The contact angles of DI water and PS beads in water on the blank Si_3N_4 surface were measured to be 8° and 6°, respectively (Fig. S1, ESI†).

2.2 Polystyrene (PS) beads in water

Two types of 1 wt% PS beads in water, one with a bead diameter of 100 nm and the other with a bead diameter of 60 nm, were purchased from Thermos Scientific and are certified as traceable to the standard meter of the National Institute of Standards and Technology. The 1 wt% 100 nm PS beads in water were diluted in DI water to 0.5 wt% and 0.1 wt% and then dispersed by using an ultrasonicator for 10 min.

2.3 Loading water into the microchannel

A 1 μL liquid sample (PS beads in water) was dropped on a glass and then transferred into a microchannel by touching the channel opening to the droplet for 1 s. When the microchannel touched the liquid sample, the liquid loaded into the microchannel by the capillary effect. To obtain a fully filled microchannel, it was sealed immediately after loading.

2.4 Forming the void (and water layers)

To obtain water layers, the microchannel was exposed to the air for as much time as was needed for the liquid to evaporate.

In our preparation protocols, the gap was filled with water. Then, the water was allowed to evaporate off to form a void. This process left behind water layers. The void between the water layers was likely directly exposed to the atmosphere outside of the channel, and should thus not be characterized as a bubble.

Notably, once the water layers form, if not sealed, they continue to vaporize and dry in a matter of minutes. However, during this vaporization process, there is no flow in the water,[21] and the particles remain in place when water layers initially form.

3. Results and discussion

In this study, we characterized water layers, as depicted in Fig. 1(b), in a microchannel (the K-kit). First, we directly measured the water thickness by using electron energy loss spectroscopy (EELS). To further study the water layer structure, we added PS beads

as nanoparticle tracers, as illustrated in Fig. 1(c) and (d). By comparing images at different tilt angles, we observed two similar water layers associated with each wall surface. By counting nanoparticles on the TEM images, we determined the water layer thickness quantitatively, which is also an independent confirmation of the EELS measurement.

As an electron beam passes through a material, some of the electrons undergo inelastic scattering with the atoms in the material, thus losing energy. By considering known scattering probabilities, one can deduce the thickness of the material from the energy loss spectrum. Fig. 2 shows three EELS spectra corresponding to an empty K-kit (in black), a K-kit with water layers (in blue), and a fully filled K-kit (in brown). Additional details on our EELS data can be found in Fig. S2 (ESI†). The EELS data showed that the amount of water in the water layers in the channel was equivalent to a total thickness of 203 ± 25 nm of water. This amount was substantially less than the amount of water necessary to fill the 2 μm channel gap height where the 0-loss peak was diminished because of the scattering of 2 μm-thick water.

The water could not be imaged using TEM; however, nanoparticles dispersed in the water could. To investigate the distribution of this amount of water in the channel, we used PS beads as tracer particles. We used PS because it is an organic compound that provides favorable TEM contrast but whose properties do not differ excessively from water. (For example, in contrast to gold nanoparticles, PS is similar to water in specific density and dielectric and optical properties). Using a microchannel in a K-kit is convenient because the observation windows on a K-kit are designed for the TEM observation of nanoparticles in liquid.

A TEM image can be considered a top view projection of the specimen. Rotating the specimen (*i.e.*, a tilted image) yields a different perspective of the specimen. The parallax effect of nano-objects reveals the relative height in the thickness dimension in the specimen. According to the image analyses shown in Fig. S3(a)–(d) (ESI†), we conclude that in our experiment there were two water layers; one adjoining each window wall. Additional details on calculating the relative heights of water layers are provided in ESI.†

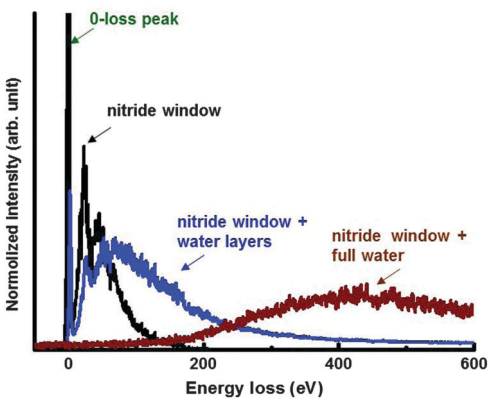

Fig. 2 The TEM EELS spectra of K-kits with channel gap heights of 2 μm. K-kit only (nitride window films only), K-kit with water layers (nitride window films and water layers), and K-kit fully filled with water (nitride window films and 2 μm-thick water).

From the known weight concentrations of the materials we used, and from the known sizes of the nanoparticles we used, we derived the number of particles per unit volume that we added into the water. By then counting the number of particles in the TEM images, we derived an area density, which is the particle number per unit area. An effective water layer thickness was obtained according to the ratio of area density to volume density, assuming that the nanoparticles were uniformly, or more precisely randomly, distributed in the liquid at all times (or, at least until the formation of a void). The thickness obtained from tracer particles is referred to as the "effective thickness" to distinguish it from the thickness obtained using EELS.

Fig. 3(a)–(c) show TEM images of nanoparticles in water layers from K-kits with different channel gap heights, of 1, 2, and 5 μm. The nanoparticle area densities were observed to be very similar despite the different channel gaps. This indicates that, despite different thicknesses of filled water, which are the gap heights, once a void formed, the water layers on the channel walls had similar thicknesses. Fig. 3(d) and (e) show TEM images for PS bead weight concentrations of 0.5 wt% and 0.1 wt% respectively, compared with the 1 wt% weight concentration in Fig. 3(b). The observed nanoparticle area density was found to be proportional to weight concentration, indicating the same effective water layer thickness. Fig. 3(f) shows an image of the same weight concentration but with a different particle size, 60 nm *versus* 100 nm in Fig. 3(b). Again, the observed nanoparticle area density was consistent with the same effective water layer thickness resulting from both particle sizes.

Fig. 4 presents a summary of the effective water layer thicknesses we tested with the aforementioned protocol. Regardless of the values of the various parameters, including channel gap height, particle concentration, and particle diameter, the thicknesses of all water layers were determined to fall within the 100–170 nm range, except for a few outliers that are not shown here. This result is consistent with the results from the EELS measurement.

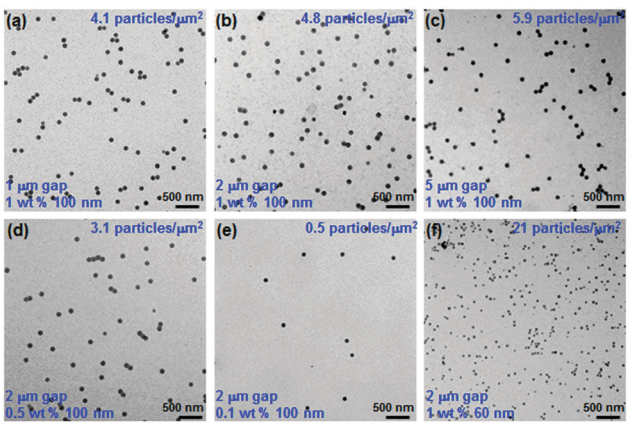

Fig. 3 TEM images of 1 wt% 100 nm PS beads in water layers inside K-kits with the gap heights of (a) 1 μm, (b) 2 μm, and (c) 5 μm. TEM images of (d) 0.5 wt% and (e) 0.1 wt% of 100 nm PS beads, and (f) 1 wt% of 60 nm PS beads in water layers inside K-kits with gap heights of 2 μm. Results of the particle density calculations indicated the presence of a 100–170 nm-thick water layer, which was found to be independent of channel gap heights and of particle sizes and concentrations.

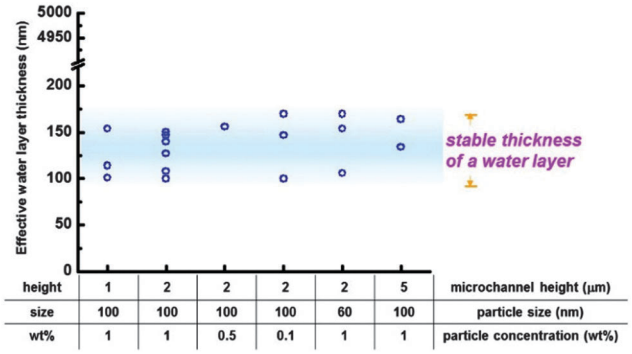

Fig. 4 Effective water layer thickness under different sample conditions, including channel gap heights, and particle sizes and concentrations.

We have observed a consistent water layer thickness. The persistence of this thickness, regardless of changes in the channel gap height, particle concentration, and particle size, rules out the scenario in which particles were drawn to the windows and remained there while the void formed (again, the amount of water is insufficient to fill the gap). Because the channel gaps were different, there were different numbers of particles at the beginning, before the void formed. The particle concentrations were obtained by diluting the purchased solution in DI water; the surfactant therein was diluted simultaneously. Thus, the layer thickness was not sensitive to the surfactant concentration either. Moreover, in our previous investigations, the LB solution[22] (1 wt% tryptone, 0.5 wt% sodium chloride, and 0.5 wt% yeast extract in DI water) and the 24 mM $CuSO_4$ solution[23] yielded water layer thicknesses of approximately 180 nm and 200 nm, respectively. These results provide evidence for the water layer thickness being independent of PS beads and its surfactant. The results also imply that the force holding the water layers to the walls was not Coulombic (*e.g.*, electrical double layer and surface charge) since the strength of such interactions would have shown a strong dependence on electrolyte concentration.

Water layers dry out when exposed to air. However, if properly sealed, water layers were stable without any special care for at least one week. The detailed observation of the formation of water layers will be the subject of future reports. We have here reported the distinct possibility of water layers of consistent thickness being markedly thicker than previously expected.

4. Conclusions

On the basis of the presented observations, we conclude that there is genuine 100–170 nm-thick stable water layer in our microchannel. Liquid surface tension and adhesion between liquids and solids have been asserted to be the dominating forces in microfluidics. We have determined that neither of these two forces favors any thickness beyond the normally short-ranged van der Waals forces. Water surface tension would minimize the surface area for a given amount of water. A thinner water layer would not diminish adhesion energy but free the water to bridge the gap, eliminating two surfaces in the bridged area and reducing the total surface area. A long-ranged (*i.e.*, >100 nm) interaction must have supported the maintenance of the observed thickness in our experiments against surface tension. We speculate that this thick water layer could have been a manifestation of the Casimir–Lifshitz effect. However, a proof of this relationship is beyond the scope of this study. Whether water cluster theory[24] supports or disfavors a thick layer remains unclear.

Our results indicate that a water layer naturally forms and associates closely with the adjacent solid surface. The possibility of such a thick water layer on a solid surface might open new possibilities in the mechanistic understanding of physical, chemical, and biological processes or in designing engineering systems that may take advantage of such a water layer or avoid its side effects.

Acknowledgements

This work is supported by the Ministry of Science and Technology, Taiwan, under project number MOST 103-2221-E-007-040. We thank Bio Materials Analysis Technology Inc. for providing the K-kit microchannel devices.

References

1 R. D. Deegan, O. Bakajin, T. F. Dupont, G. Huber, S. R. Nagel and T. A. Witten, *Nature*, 1997, **389**, 827–829.
2 P. J. Yunker, T. Still, M. A. Lohr and A. G. Yodh, *Nature*, 2011, **476**, 308–311.
3 J. Thomson, *Philos. Mag.*, 1855, **10**, 330–333.
4 H. J. Lee and S. Michielsen, *J. Text. Inst.*, 2006, **97**, 455–462.
5 M. Yamamoto, N. Nishikawa, H. Mayama, Y. Nonomura, S. Yokojima, S. Nakamura and K. Uchida, *Langmuir*, 2015, **31**, 7355–7363.
6 A. Lafuma and D. Quere, *Nat. Mater.*, 2003, **2**, 457–460.
7 W. S. N. Trimmer, *Sens. Actuators*, 1989, **19**, 267–287.
8 F. London, *Trans. Faraday Soc.*, 1937, **33**, 8–26.
9 W. Sparreboom, A. V. D. Berg and J. C. T. Eijkel, *New J. Phys.*, 2010, **12**, 015004.
10 J. Israelachvili and D. Tabor, *Proc. R. Soc. London, Ser. A*, 1972, **331**, 19–38.
11 G. Palasantzas, V. B. Svetovoy and P. J. van Zwol, *Phys. Rev. B: Condens. Matter Mater. Phys.*, 2009, **79**, 235434.
12 D. Ganta, E. B. Dale and A. T. Rosenberger, *Meas. Sci. Technol.*, 2014, **25**, 055206.
13 D. O. Shah, *Thin Liquid Films and Boundary Layers: Special Discussion of the Faraday Society*, Academic press, New Work, 1971.
14 J. Bastacky, C. Y. C. Lee, J. Goerke, H. Koushafar, D. Yager, L. Kenaga, T. P. Speed, Y. Chen and J. A. Clements, *J. Appl. Physiol.*, 1995, **79**, 1615–1628.
15 R. E. Pattle, *Nature*, 1955, **175**, 1125–1126.
16 E. R. Weibel and J. Gil, *Respir. Physiol.*, 1968, **4**, 42–57.
17 H. B. G. Casimir, *Proc. K. Ned. Akad. Wet., Ser. C: Biol. Med. Sci.*, 1948, **51**, 793–795.
18 T. A. Siebert and S. Rugonyi, *Biophys. J.*, 2008, **95**, 4549–4559.
19 B. Olmeda, L. Villen, A. Cruz, G. Orellana and J. Pereze-Gil, *Biochim. Biophys. Acta*, 2010, **1798**, 1281–1284.

20 K. L. Liu, C. C. Wu, Y. J. Huang, H. L. Peng, H. Y. Chang, P. Chang, L. Hsu and T. R. Yew, *Lab Chip*, 2008, **8**, 1915–1921.
21 L. A. Tai, Y. T. Kang, Y. C. Chen, Y. C. Wang, Y. J. Wang, Y. T. Wu, K. L. Liu, C. Y. Wang, Y. F. Ko, C. Y. Chen, N. C. Huang, J. K. Chen, Y. F. Hsieh, T. R. Yew and C. S. Yang, *Anal. Chem.*, 2012, **84**, 6312–6316.
22 K. L. Liu, PhD thesis, National Tsing-Hua University, 2010.
23 S. E. Lai, Y. J. Hong, Y. T. Chen, Y. T. Kang, P. Chang and T. R. Yew, *Microsc. Microanal.*, 2015, **21**, 1639–1643.
24 U. Buck, C. C. Pradzynski, T. Zeuch, J. M. Dieterich and B. A Hartke, *Phys. Chem. Chem. Phys.*, 2014, **16**, 6859–6871.
25 H. W. Chen, R. Gouk, S. Verhaverbeke and R. J. Visser, *ECS Trans.*, 2013, **58**, 205–211.
26 N. Sato, *Microelectron. Eng.*, 2015, **134**, 38–42.